

Stimulation of Actin ATPase Activity by Cytochalasins Provides Evidence for a New Species of Monomeric Actin*

(Received for publication, March 12, 1981)

Stephen L. Brenner[‡] and Edward D. Korn[§]

From the [‡]Physical Sciences Laboratory, Division of Computer Research and Technology and the [§]Laboratory of Cell Biology, National Heart, Lung, and Blood Institute, National Institutes of Health, Bethesda, Maryland 20205

The ATPase activities of *Acanthamoeba* and muscle actins in 0.5–0.6 mM MgCl₂ were examined below and above their critical concentrations and in the presence and absence of cytochalasins B, C, D, and E. In the absence of cytochalasin, the ATPase activity of actin solutions at steady state increased with increasing actin concentration through the critical concentration and continued to increase as the concentration of F-actin increased. Cytochalasin D stimulated the ATPase of actin monomer about 30-fold below its critical concentration; the stimulated ATPase rate was linear with actin concentration and no actin oligomers were detected. Above the critical actin concentration, the cytochalasin-stimulated ATPase rate was constant and independent of the F-actin concentration. Double reciprocal plots of cytochalasin-stimulated actin ATPase activity as a function of total cytochalasin concentration were linear for both actins, below their critical concentrations, for all four cytochalasins tested, indicating that essentially all of the cytochalasin was free. The values of V_{\max} for the four cytochalasins were very similar for each actin, varying at most by a factor of 2, while the K_{app} values varied by as much as 400-fold. A simple model that can explain these and other experimental data requires the existence in the ATPase cycle of low concentrations of an intermediate between actin-ATP and actin-ADP to which cytochalasins bind weakly, rapidly, and reversibly. In the absence of cytochalasins, the disappearance of this intermediate would be the rate-limiting step. Cytochalasins would stimulate this step making the rate of formation of the intermediate rate-limiting. Cytochalasins, therefore, might affect actin polymerization by direct interaction with monomeric actin in addition to their tight binding to ends of filaments.

The ability of the cell to control the polymerization and depolymerization of actin filaments and the assembly of filaments into cross-linked networks seems to be vital to a variety of motile events (1). Considerable progress has been made recently in identifying proteins that affect actin polymerization (2–10) and depolymerization (11–14), proteins that cross-link F-actin (15–21), and proteins that affect dissolution of filament networks (8, 9, 22, 23). To understand how these proteins function, it will be necessary to have a fuller understanding of the molecular events in the polymerization of actin in the absence of such accessory proteins.

The actin protomer, G-actin, is a slightly asymmetric mol-

ecule (24) with a molecular weight of 42,000 (25). G-actin contains a single nucleotide-binding site which binds ATP ($K_D = 10^{-10}$ M) 100 times more tightly than ADP ($K_D = 10^{-8}$ M) (26) and a single high affinity divalent cation-binding site (27) with almost equal affinity for Mg²⁺ ($K_D = 35$ μ M) and Ca²⁺ ($K_D = 10$ μ M) (28). Under physiological conditions, then, ATP should occupy the nucleotide-binding site and Mg²⁺ should occupy the divalent cation-binding site of G-actin.

Purified G-actin is stable in buffers of low ionic strength that contain ATP or ADP and divalent cation, typically 100 μ M Ca²⁺. Upon addition of salt, usually 50–100 mM KCl or 0.5–2.0 mM MgCl₂, G-actin polymerizes to polar helical filaments of F-actin that contain hundreds or thousands of protomers. Polymerization continues until the concentration of monomeric G-actin falls to its critical concentration. The rate of polymerization and the steady state distribution of actin between monomers and filaments are determined by the ionic conditions and temperature (1).

The polymerization of G-actin-ATP is normally accompanied by hydrolysis of the actin-bound ATP so that the filaments of F-actin contain, predominantly, bound ADP (29). At least under some conditions, the ATP is probably hydrolyzed subsequent to the addition of monomeric actin to the filament (30) and, when polymerization is induced by KCl, hydrolysis of ATP may lag significantly behind polymerization (31, 32). Possibly under all, or most, conditions of polymerization, at least one end of the filament may contain a protomer with a bound ATP (30, 31). Covalently cross-linked actin dimers, prepared from F-actin and possibly in an F conformation, bind ATP more tightly than ADP (33).

Monomeric actin with bound ADP (34), or nonhydrolyzable analogues of ATP (35), also polymerizes, however, and the role of the hydrolysis of ATP that presumably accompanies actin polymerization *in vivo* is not understood. It may be related to the fact that the irreversible hydrolysis of ATP makes the polymerization of actin a steady state, rather than an equilibrium, reaction so that the critical concentrations at the two ends of the filament can be different (36). As a consequence, the filament at steady state can have a net polymerizing end and a net depolymerizing end. This could not occur, of course, if one end of the filament were blocked or associated with another structure, as may be the case *in vivo*.

The cytochalasins are a group of fungal metabolites that affect a wide variety of cellular movements (37) and have pronounced effects on actin polymerization (31, 38–41) and actin filament network formation (41, 42) *in vitro*. These properties of the cytochalasins can largely be explained by their high affinity binding to at least one end of the actin filament (38–42), that which would otherwise have been the net polymerizing end at steady state. As a consequence of the binding of cytochalasins to filament ends, the concentration

* The costs of publication of this article were defrayed in part by the payment of page charges. This article must therefore be hereby marked "advertisement" in accordance with 18 U.S.C. Section 1734 solely to indicate this fact.

of polymerized actin at steady state may be lowered (38), the filaments may become shorter (42), and postulated interactions between filaments may be blocked (41). The magnitude of a particular response will depend on the specific cytochalasin used and the ionic conditions.

Cytochalasins have also been shown to stimulate the ATPase activity of solutions of F-actin (43, 44). This phenomenon is usually attributed to a general destabilization of the filaments, i.e. a higher steady state turnover rate. Recently, we showed that cytochalasin D also greatly stimulates an ATPase activity of monomeric G-actin that occurs, even in the absence of cytochalasin, in solutions containing 0.5 mM Mg^{2+} (31). We proposed that cytochalasin D interacts with monomeric actin and accelerates the rate-determining step in the hydrolysis of ATP by G-actin. To our knowledge, this is the only evidence for the interaction of cytochalasins with monomeric actin, an interaction that has not been detected by direct binding studies (40). It should be noted, however, that Selden and co-workers (45, 46) have interpreted related data in a different way that does not postulate hydrolysis of ATP by monomeric actin.

We have now examined in more detail the effects of cytochalasins B, C, D, and E on the steady state ATPase activities of muscle and *Acanthamoeba* actins below and above their critical concentrations. In all situations, all of the cytochalasin-stimulated hydrolysis of ATP can be attributed to the activity of monomeric actin. At a minimum, these results require the existence of G-actin·ADP·P_i as an intermediate between G-actin·ATP and G-actin·ADP + P_i. Since the ATPase activity of monomeric actin is expressed under normal polymerizing conditions, in the absence as well as the presence of cytochalasins, intermediates in the actin ATPase cycle must also be considered as possible intermediates in the polymerization of G-actin·ATP to F-actin. In addition, the kinetic evidence for the interaction of cytochalasins with monomeric actin suggests that previous interpretations of the effects of cytochalasins on actin polymerization may have been incomplete in that they considered only the interaction of cytochalasins with F-actin.

MATERIALS AND METHODS

ATP, imidazole and β -mercaptoethanol were purchased from Sigma Chemical Co.; cytochalasins B, C, D, and E were from Aldrich Chemical Co.; and AMP-PNP¹ was from P-L Biochemicals. Stock solutions of cytochalasins were prepared in dimethylsulfoxide and stored at 5 °C. [α -³²P]ATP and [γ -³²P]ATP (2–10 Ci/mmol) from New England Nuclear were diluted immediately upon arrival to 0.5 mCi/ml in 2 mM ATP and stored at –20 °C. The radiochemical purity of the [γ -³²P]ATP was 85–95% as determined by the percentage of total radioactivity hydrolyzed to P_i by myosin (47), and the radiochemical purity of the [α -³²P]ATP was 86–92%, as determined chromatographically (33). All specific activities were corrected accordingly.

Muscle G-actin was prepared from acetone powders of rabbit back and leg muscle by the method of Spudich and Watt (48) as modified by Eisenberg and Kielley (49). Purified covalently cross-linked muscle actin dimer (33) was obtained from Dr. Stephen Mockrin. *Acanthamoeba* G-actin was isolated by the procedure of Gordon *et al.* (50). The concentrations of monomeric actins were determined either from their absorbances at 290 nm, using an extinction coefficient of 0.617 mg^{–1} ml cm^{–1} (51), or by the procedure of Lowry *et al.* (52), using muscle G-actin as standard. Both preparations of G-actin were stored in buffer consisting of 3 mM imidazole chloride, pH 7.5, 0.1 mM CaCl₂, 0.5 mM ATP, 0.75 mM β -mercaptoethanol and 0.01% NaN₃ (Buffer G).

G-actin was labeled with radioactive ATP, and the bound nucleotide (0.9–1.0 mol of ATP/mol of actin) and total exchangeable nucleotide (typically 0.93 mol of ATP/mol of actin) were determined as described previously (31). Hydrolysis of [γ -³²P]ATP was followed by

measuring the release of ³²P_i (47). Light scattering measurements were made using a Hitachi MPF-2A fluorescence spectrophotometer at a 90° scattering angle with excitation and emission wavelengths of 350 nm. Nonsedimentable actin was determined after centrifugation in a Beckman Airfuge at room temperature for 30 min at 178,000 × g.

RESULTS

Effect of Cytochalasin D on the Steady State Hydrolysis of ATP by Actin—We had previously observed (31) that the cytochalasin-stimulated hydrolysis of ATP occurred below the critical concentration of actin, where only monomeric G-actin should have been present, and that the initial rates of ATP hydrolysis, both below and above the critical concentration, were directly proportional to the actin concentration and, therefore, apparently independent of actin-actin interactions. These studies have now been extended to measurements of the steady state actin ATPase activity as a function of actin concentration above and below the critical concentration and in the presence and absence of cytochalasin D.

In the experiment described in detail in the legend to Fig. 1, actin was added over a wide range of concentrations to Buffer G containing 0.5 mM MgCl₂ and allowed to polymerize overnight to steady state. Aliquots were then removed to determine the concentration of nonpolymerized actin by the centrifugation assay. A critical concentration of 5 μ M (Fig. 1A) was obtained which was in reasonable agreement with the value of 4 μ M obtained for the same preparation of actin by viscometry. At the same time, the rates of ATP hydrolysis were measured and were found to be approximately proportional to the actin concentration over the entire range examined. The important aspect of this experiment, however, is that the rate of hydrolysis of ATP continued to increase with actin concentration above the critical concentration when only the concentration of F-actin was increasing. This must mean that most of the ATPase activity under these conditions was due either to filament turnover, or to the interaction of a constant concentration of actin monomer with an increasing concentration of filament ends, or both.

When 1 μ M cytochalasin D was added to the same solutions of actin, and time was allowed for the new steady state to be reached, the critical concentration increased to about 8 μ M (Fig. 1B). A similar increase in critical concentration was observed by viscometry (38). No evidence for the presence of actin oligomers, below the critical concentration, was obtained by light scattering measurements, under conditions in which cross-linked actin dimer gave twice the signal as an equal weight of monomer.

Below the critical actin concentration, the steady state rate of ATP hydrolysis was 30 times greater in the presence of cytochalasin D than in its absence and was directly proportional to the actin concentration (Fig. 1B). More importantly, however, as the actin concentration was increased above its critical concentration, the rate of hydrolysis of ATP remained constant and equal to the rate observed at the critical concentration despite the increasing concentration of F-actin. These data provide strong additional evidence that the cytochalasin-stimulated hydrolysis of ATP is entirely due to monomeric actin with no significant contribution from either polymer turnover or the interaction of actin monomers with filament ends. Furthermore, the steady state hydrolysis of ATP that, in the absence of cytochalasin, is coupled to the interaction of G-actin and F-actin (Fig. 1A) is apparently inhibited by cytochalasin D (Fig. 1B), presumably because of the binding of cytochalasin to filament ends.

Kinetic Analysis of the Cytochalasin-stimulated Steady State ATPase Activity of Actin Monomer—Although the stimulation of monomeric actin ATPase activity by cytocha-

¹ The abbreviations used are: AMP-PNP, adenylyl-5'-yl imidodiphosphate; EGTA, ethylene glycol bis(β -aminoethyl ether)-N,N',N'',N'-tetraacetic acid.

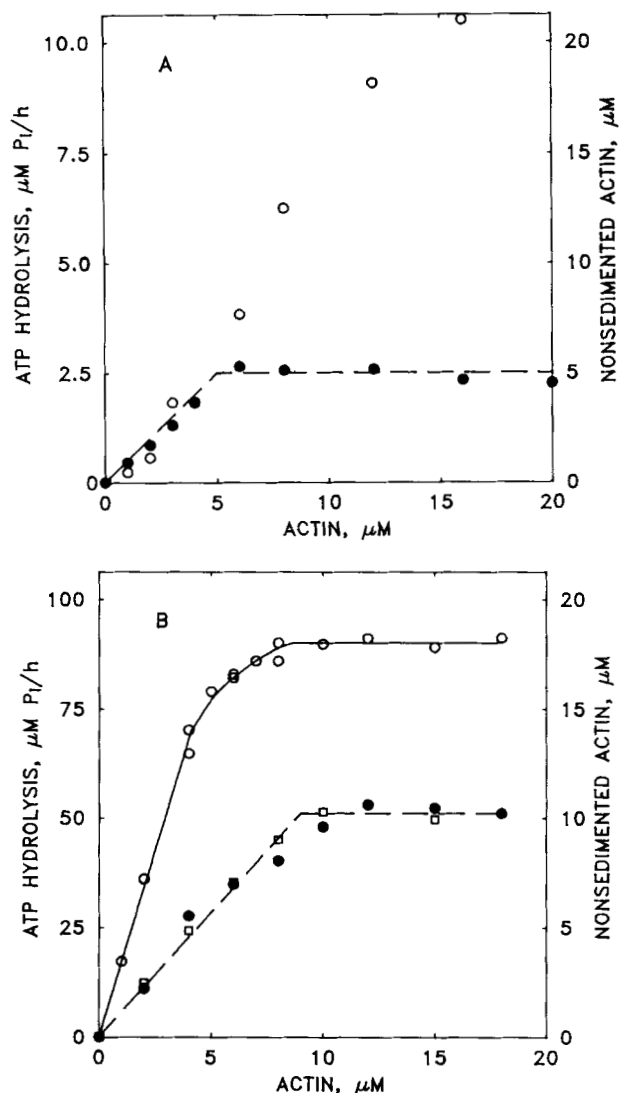


FIG. 1. Effect of cytochalasin D on the hydrolysis of ATP as a function of actin concentration. *Acanthamoeba* actin was labeled with $[\gamma\text{-}^{32}\text{P}]\text{ATP}$ as described (31), diluted to the concentrations shown, and polymerized overnight (17 h) at 27 °C in Buffer G containing 250 μM $[\gamma\text{-}^{32}\text{P}]\text{ATP}$ and 0.6 mM MgCl_2 . Either 1% dimethylsulfoxide (A) or 1 μM cytochalasin D, 1% dimethylsulfoxide (B) was then added and the samples were incubated an additional 15 min at 27 °C. The nonsedimentable actin (●, □) in each sample was determined by spinning 150- μl aliquots at $178,000 \times g$ in a Beckman Airfuge for 30 min and assaying the protein in the supernatant by the method of Lowry *et al.* (52). The linear ATPase activity (○) was followed for 7.5 h (A) or 60 min (B). For the cytochalasin-treated samples (B), nonsedimentable actin was determined both before (●) and after (□) the ATPase assay (○) to be sure that no change in the distribution of G-actin and F-actin occurred during the 1-h incubation.

lasin requires interaction between the two, several different direct attempts to measure the binding of cytochalasins to actin monomer were unsuccessful. Equilibrium dialysis failed to detect any binding between $[\text{H}]\text{cytochalasin B}$ and G-actin·ATP, G-actin·ADP, or G-actin·AMP-PNP in Buffer G, with or without 0.5 mM MgCl_2 , and cytochalasin D produced no measureable effect on the intrinsic fluorescence spectrum of G-actin·ATP in Buffer G containing 0.5 mM MgCl_2 .

The reason why binding could not be demonstrated directly became apparent from kinetic analysis of the effects of cytochalasins on the actin ATPase activity. Double reciprocal plots of the cytochalasin-stimulated ATPase activity per actin monomer as a function of cytochalasin concentration were

linear for both muscle and *Acanthamoeba* actin below their critical concentrations for all four cytochalasins tested (Fig. 2, A and B). The fact that these curves were linear with respect to the total cytochalasin concentration means that essentially all of the cytochalasin was free, *i.e.* not bound to actin, even at points very close to V_{max} , where, for example, the molar

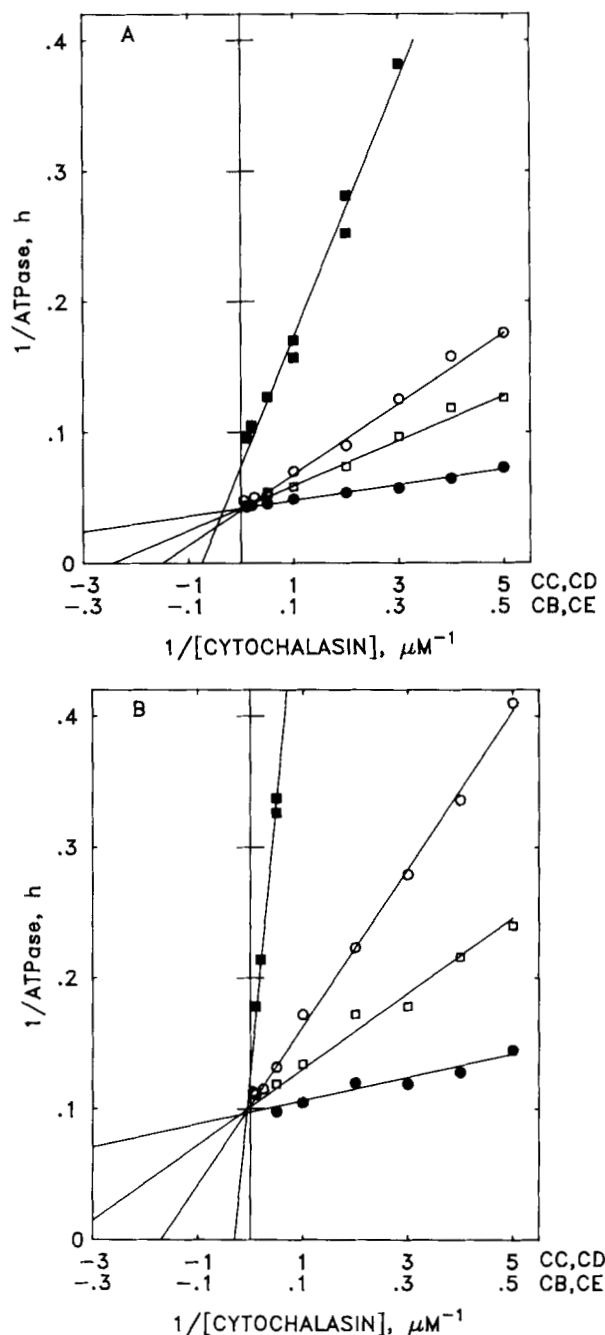


FIG. 2. Double reciprocal plot of G-actin ATPase activity as a function of the concentrations of cytochalasin B, C, D, and E. Samples of *Acanthamoeba* actin (A) or muscle actin (B) were prepared in concentrations of 2 μM in Buffer G containing 100 μM $[\gamma\text{-}^{32}\text{P}]\text{ATP}$ and 0.5 mM MgCl_2 . Cytochalasins B (○), C (□), D (●), or E (■) were added from stock solutions to keep the final dimethylsulfoxide concentration at 1% in all samples. ATP hydrolysis was monitored at 30 °C and was linear with time for at least 60 min. The ATPase rate is calculated as moles of P_i /mol of actin/h. The ATPase activity in the absence of cytochalasin (V_0) was subtracted from the rates in the presence of the cytochalasins. Note that the scale on the abscissa for cytochalasins B and E (CB, CE) is different from that for cytochalasins C and D (CC, CD).

ratio of cytochalasin D to monomeric actin was 1:1 (Fig. 2A) or 2:1 (Fig. 2B).

This point is more clearly made in the experiment shown in Fig. 3, which is a double reciprocal plot of the cytochalasin D-stimulated ATPase activity per cytochalasin as a function of actin concentration. If essentially all of the cytochalasin were free, the cytochalasin-stimulated ATPase rate per cytochalasin should be proportional to the actin concentration but, if the cytochalasin became saturated with actin, the rate would level off as the actin concentration was increased. The *solid line* in Fig. 3 shows a double reciprocal plot of the cytochalasin-stimulated ATPase rate per actin monomer as a function of cytochalasin concentration similar to the curves in Fig. 2. The *dashed lines* in Fig. 3 show the theoretical curves at four fixed cytochalasin concentrations if the ATPase rates per cytochalasin were linearly proportional to the actin concentration. The experimental data agreed very well with the theoretical curves, demonstrating that essentially all of the cytochalasin was free.

The values for V_{\max} and K_{app} from Fig. 2 are summarized in Table I. The V_{\max} values obtained with all four cytochalasins were very similar for both actins. They varied by only 20% with muscle actin and, with *Acanthamoeba* actin, the V_{\max} values were identical for three cytochalasins while the value for cytochalasin E differed by only a factor of 2. The values for K_{app} , on the other hand, varied by as much as 400-fold (compare cytochalasin D and E with muscle actin), although they were in the same relative order of activity for the two actins. The full implications of these data will be developed in the "Discussion" and the "Appendix." It is of interest to note, however, that the K_{app} for cytochalasin D is about 0.1 μM when the concentration of monomeric actin is 2 μM , so that most of the actin, as well as the cytochalasin, must be free

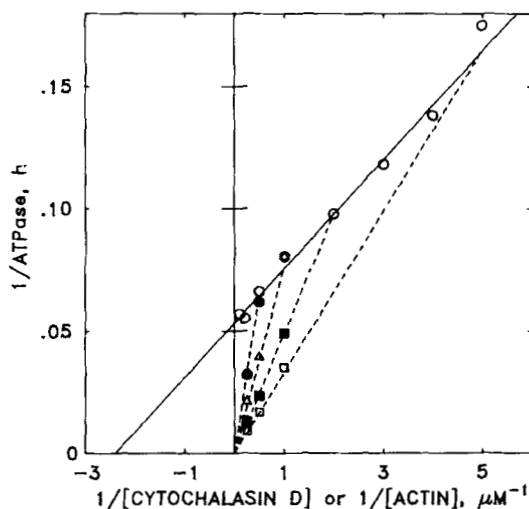


FIG. 3. Double reciprocal plots of cytochalasin-stimulated G-actin ATPase activity as a function of the concentration of either cytochalasin or actin. Samples of *Acanthamoeba* actin were prepared in Buffer G containing 150 μM [$\gamma\text{-}^{32}\text{P}$]ATP and 0.5 mM MgCl_2 . Cytochalasin D was added from stock solutions to keep the final dimethylsulfoxide concentration at 1% in all samples. ATP hydrolysis at 30 °C was linear with time for the 60-min experiment. The *solid curve* (○) shows the results at a fixed actin concentration (1 μM) when the cytochalasin concentration was varied. The ATPase rate is calculated as moles of P_i /mol of actin/h. In the other experiments, the actin concentration was varied with the cytochalasin D concentration constant at 2 (●), 1 (△), 0.5 (■), or 0.2 (□) μM , and the ATPase activity is calculated as moles of P_i /mol of cytochalasin/h. The *dashed curves* show what would theoretically occur, in such experiments, if the ATPase rate per cytochalasin were directly proportional to the actin concentration.

TABLE I

Kinetic parameters for cytochalasin-stimulated hydrolysis of ATP by monomeric actin

V_{\max} and K_{app} values obtained from double reciprocal plots such as those in Fig. 2 are summarized below. The buffer contained 3 mM imidazole-Cl, 0.1 mM CaCl_2 , 0.5 mM MgCl_2 , 0.1 mM [$\gamma\text{-}^{32}\text{P}$]ATP, 1% dimethylsulfoxide and 0.01% NaN_3 , pH 7.5, unless otherwise noted. The stock solution of G-actin in Buffer G was prelabeled by overnight incubation with [$\gamma\text{-}^{32}\text{P}$]ATP at the same specific activity as that used in the experiment. All measurements were performed at 30 °C. The rate in the absence of added cytochalasin (V_0) was subtracted from the rates in the presence of cytochalasin. V_0 was 0.2–0.3 mol of P_i /mol of actin/h for muscle actin and 0.4–0.6 mol of P_i /mol of actin/h for *Acanthamoeba* actin.

Cytochalasin	Muscle actin		<i>Acanthamoeba</i> actin	
	K_{app} μM	V_{\max} mol P_i /mol actin/h	K_{app} μM	V_{\max} mol P_i /mol actin/h
B	5.6	9.4	6.7	24.0
C	0.30	10.0	0.43	23.0
D	0.08	10.1	0.14	24.0
E	33.0	8.0	10.0	12.0
B ^a	22.0	9.8	29.0	22.0
D ^a	0.23	11.1	0.53	22.1
D ^b			0.23	19.0
D ^c			0.14	25.0

^a ATP concentration, 240 μM ; all other conditions as above.

^b ATP concentration, 80 μM ; other conditions as above, $V_0 = 0.45$ mol of P_i /mol of actin $^{-1}$ h $^{-1}$.

^c ATP concentration, 80 μM , 1 mM EGTA added; other conditions as above, $V_0 = 1.24$ mol of P_i /mol of actin $^{-1}$ h $^{-1}$.

when the cytochalasin-stimulated ATPase activity has reached half its maximal rate.

Increasing the concentration of ATP, and thereby lowering the free Mg^{2+} concentration, had no significant effect on the V_{\max} values for either cytochalasin B or cytochalasin D with muscle or *Acanthamoeba* actins, but the K_{app} values did increase (Table I). Addition of 1 mM EGTA, to chelate all of the Ca^{2+} , did not have a significant effect on either the V_{\max} or K_{app} values of the cytochalasin-stimulated ATPase activity of *Acanthamoeba* actin, but it did increase the rate of ATP hydrolysis in the absence of cytochalasin (V_0) by a factor of about 2–3 (Table I).

In contrast to the linearity of the plots at the cytochalasin concentrations used for the experiments in Fig. 2, double reciprocal plots of cytochalasin-stimulated ATPase activity per actin monomer did differ significantly from linearity at concentrations of cytochalasin D very much greater than K_{app} (Fig. 4). High concentrations of cytochalasin D reduced the cytochalasin-stimulated ATPase activity of *Acanthamoeba* actin and stimulated the activity of muscle actin relative to the extrapolated V_{\max} values. In neither case, however, did the ATPase rate at the maximal concentration of cytochalasin tested, which was limited by solubility, differ from the V_{\max} by more than a factor of 2.

Possible Intermediates in the Hydrolysis of Actin-bound ATP—At a minimum, the hydrolysis of ATP to ADP catalyzed by actin must involve the intermediate formation of actin·ATP, actin·ADP· P_i , and actin·ADP, assuming that bound P_i is released before bound ADP. Actin·ADP· P_i will accumulate in detectable amounts if the rate of product release from the actin is less than the rate of hydrolysis of actin-bound ATP and if the equilibrium, $\text{actin} \cdot \text{ATP} \rightleftharpoons \text{actin} \cdot \text{ADP} \cdot \text{P}_i$, lies sufficiently to the right. If these conditions apply, the initial rate of hydrolysis, up to a maximum of 1 mol of ATP hydrolyzed per mol of actin, will be greater than the steady

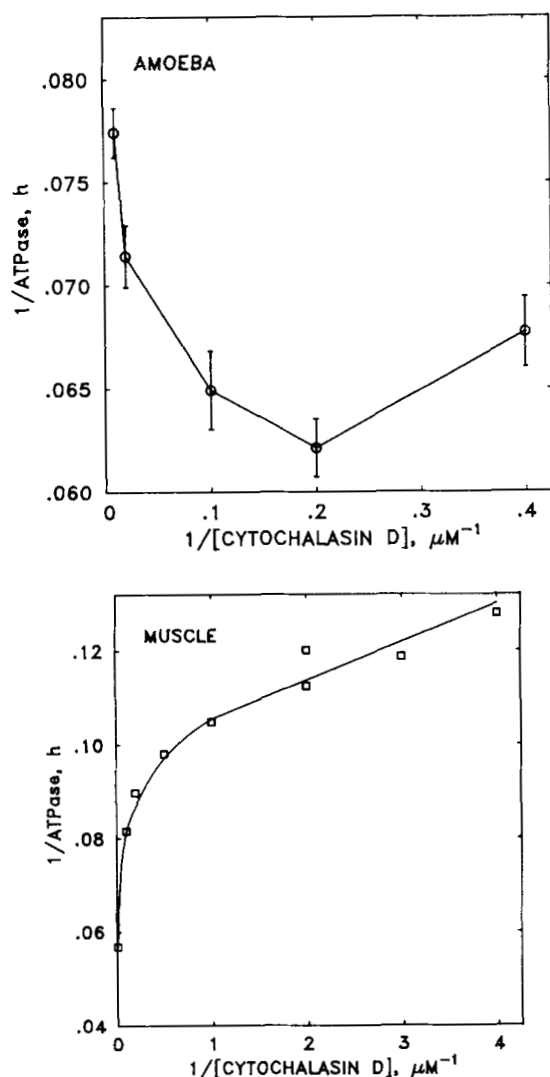


FIG. 4. Double reciprocal plots of G-actin ATPase activity as a function of cytochalasin D concentration at high concentrations of cytochalasin D. ATP hydrolysis at high concentrations of cytochalasin D was measured for *Acanthamoeba* actin (1, 2, and 4 μM) and muscle actin (2 μM) at 30 °C. The average rate per μM actin (± 1 S.D.) is plotted for *Acanthamoeba* actin. Conditions were the same as described in the legend to Fig. 2, except that the ATP concentrations were 120 μM and 150 μM for *Acanthamoeba* actin and muscle actin, respectively.

state rate of hydrolysis, because the assay for P_i does not distinguish between free and actin-bound P_i . In fact, no experimental evidence for such an initial burst of P_i formation was obtained, either in the presence or absence of cytochalasin (Fig. 5).

In the presence of excess ATP, the only actin-bound nucleotide that could be detected was ATP, both in the absence (33) and presence of cytochalasin. This is in accordance with the known affinities of ATP and ADP for actin (26). On the other hand, when cytochalasin-stimulated hydrolysis of actin-bound ATP was allowed to go to completion in the absence of free ATP (Table II), almost all of the product ADP remained bound to the actin (as measured by the radioactivity derived from $[\alpha\text{-}^{32}\text{P}]\text{ATP}$), but no actin-bound P_i could be detected (as measured by the radioactivity derived from $[\gamma\text{-}^{32}\text{P}]\text{ATP}$). In addition, excess added P_i has no effect on the rate of hydrolysis of actin-bound ATP even in the absence of free ATP. The measured rate of hydrolysis of 2 μM G-actin·ATP in Buffer G containing 0.5 mM MgCl_2 was 0.2 mol of P_i /mol of

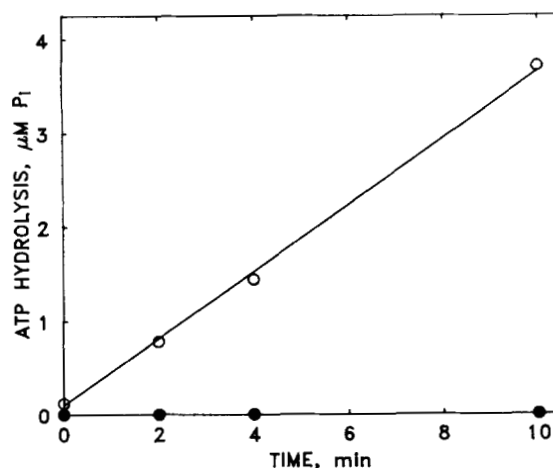


FIG. 5. Initial rate of cytochalasin-stimulated ATP hydrolysis by monomeric actin. *Acanthamoeba* actin (1 μM) was equilibrated with 80 μM $[\gamma\text{-}^{32}\text{P}]\text{ATP}$ in Buffer G containing 0.5 mM MgCl_2 . Either 1% dimethylsulfoxide (●) or 3 μM cytochalasin D, 1% dimethylsulfoxide (○) was added and ATP hydrolysis was monitored at 30 °C.

TABLE II

Bound nucleotide content of monomeric actin before and after cytochalasin-stimulated hydrolysis of ATP

Samples of *Acanthamoeba* actin (24 μM) in Buffer G were labeled with $[\alpha\text{-}^{32}\text{P}]\text{ATP}$ or $[\gamma\text{-}^{32}\text{P}]\text{ATP}$ as described (31) and freed of unbound nucleotide by addition of three consecutive aliquots (10% by volume) of 50% Dowex 1-X8 in Buffer G. After addition of each aliquot, the resin was removed by centrifugation at $3000 \times g$ for 1–2 min. The protein concentration (about 18 μM) in the final supernatant was determined from the A_{290} , and the nucleotide content was determined by scintillation counting. The labeled nucleotide-free actin was diluted to 4 μM in 0.5 mM MgCl_2 , 10 μM cytochalasin D, 1% dimethylsulfoxide, 3 mM imidazole-Cl, 0.1 mM CaCl_2 , pH 7.5, and hydrolysis of the bound ATP at 30 °C was monitored by $^{32}\text{P}_i$ release from $[\gamma\text{-}^{32}\text{P}]\text{ATP}$. Hydrolysis was complete (96%) within 15 min. After an additional 15 min, 0.5-ml samples were rapidly freed of unbound nucleotide. The protein concentration in the final supernatant was determined by the method of Lowry *et al.* (52) and aliquots were counted for radioactivity. Actin-bound radioactivity after hydrolysis in the sample that originally contained $[\gamma\text{-}^{32}\text{P}]\text{ATP}$ represented actin-bound ADP and actin-bound radioactivity in the sample that originally contained $[\alpha\text{-}^{32}\text{P}]\text{ATP}$ represented actin-bound P_i .

Labeled nucleotide	Actin-bound nucleotide or P_i	
	Before hydrolysis	After hydrolysis
<i>mol/mol actin</i>		
$[\alpha\text{-}^{32}\text{P}]\text{ATP}$	0.96	0.72
$[\gamma\text{-}^{32}\text{P}]\text{ATP}$	0.95	0.01

actin/h, in the presence and absence of 50 μM P_i . Therefore, the irreversible release of actin-bound P_i occurs before the release of actin-bound ADP.

DISCUSSION

The scheme shown in Fig. 6 is a simple model for the monomeric actin ATPase cycle that can explain the experimental data. In this scheme, $\text{ACTIN}^* \cdot \text{NUC}$ must include the species actin·ADP· P_i but may also include either a transition species, actin ‡ ·ATP, that precedes the hydrolysis step, or a transition species, actin ** ·ADP· P_i , that follows hydrolysis but precedes P_i release, or both.

In the absence of cytochalasin, hydrolysis of ATP would occur along pathway I with either step 2 or a transition occurring between steps 1 and 2 as the very slow rate-determining step. Steps 3 and 4 would be very much faster than step 2, thus explaining the inability to detect an actin·ADP

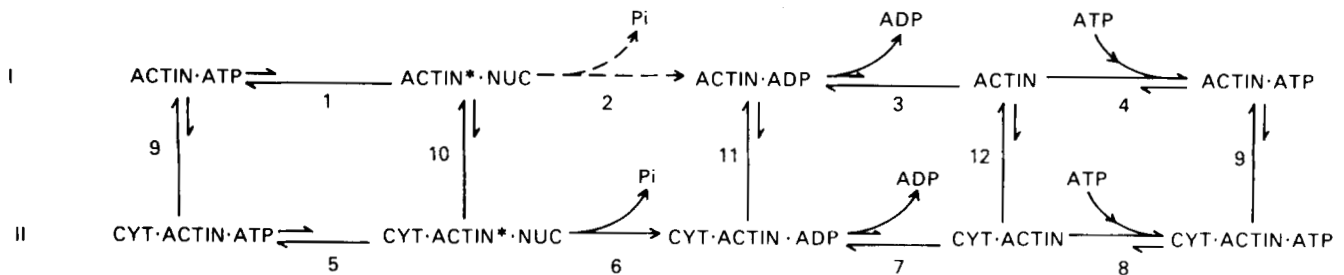


FIG. 6. Schematic representation of the proposed model for the monomeric actin ATPase cycle. In the absence of cytochalasin, ATP hydrolysis will proceed by *pathway I* with *step 2* or a transition occurring between *steps 1* and *2* as the very slow, rate-determining step, with *steps 3* and *4* very much faster than *step 2*, and with the equilibrium at *step 1* very much in favor of *ACTIN·ATP*. Cytochalasins stimulate ATP hydrolysis if *steps 10*, *6*, and *11*, for example, are

faster than *step 2*. At very high concentrations of cytochalasins, ATP hydrolysis will proceed by *pathway II*, in which *step 5* probably becomes rate-limiting. The model is presented in greater detail in the "Discussion" and "Appendix." *CYT*, cytochalasin, and *ACTIN*·NUC*, one or more species of actin-bound nucleotides, including actin·ADP·P_i.

species, in the presence of excess ATP. The equilibrium at *step 1* would lie very much in favor of actin·ATP, thus explaining the inability to detect an actin·ADP·P_i species.

According to this model, cytochalasins would stimulate the hydrolysis of ATP by binding weakly, rapidly, and reversibly to monomeric actin and stimulating the rate-determining step. This would occur, for example, if the pathway represented by steps 10, 6, and 11, or any other cytochalasin-dependent alternate route back to actin·ATP, were faster than *step 2*. *Step 1* would then become the rate-limiting reaction. Because the binding of cytochalasins is very weak, it will be difficult to detect and, because the concentration of *ACTIN*·NUC* is always very low, only a very small fraction of the total actin need be bound to cytochalasin, even very near *V*_{max}, to accelerate the rate of ATP hydrolysis. Since *V*_{max}, in the presence of cytochalasin, is determined by *step 1*, which occurs before cytochalasins bind, it will be independent of which cytochalasin is used to stimulate hydrolysis. *K*_{app}, however, will depend on the cytochalasin because it is a complex function of the binding constant for the cytochalasin and several rate constants (see "Appendix").

Again, according to the model in Fig. 6, as the concentration of cytochalasin is increased well past *K*_{app}, eventually all of the actin will be bound to cytochalasin, steps 9–12, and ATP will be hydrolyzed only by pathway II. *Step 5* will now replace *step 1* as the rate-determining step, if *step 6* is faster than *step 5*, and deviations from linearity of the double-reciprocal plots are to be anticipated. Inhibition will occur, as observed in Fig. 4A, if *step 5* is slower than *step 1*, and acceleration will occur, as observed in Fig. 4B, if *step 5* is faster than *step 1*. A more detailed kinetic analysis of the model is presented in the "Appendix."

The key feature of the proposed reaction scheme is the species *ACTIN*·NUC* which, as stated above, could represent more than one form of actin-bound nucleotide and their interconversions. For the myosin and actomyosin ATPase cycles, which provided the basis for the development of our kinetic model (53), for example, the rate-determining step for myosin alone is the very slow release of P_i from myosin·ADP·P_i, while for actomyosin, P_i release is very much faster, and the rate-determining step appears to become the posthydrolysis transition of one conformation of myosin·ADP·P_i to another before the release of myosin-bound P_i. Ferri *et al.* (54) have demonstrated the occurrence of monomeric actin·ADP·P_i in the protamine-stimulated hydrolysis of ATP, and Mockrin and Korn (33) have shown that 15% of the nucleotide bound to one of the two sites of cross-linked actin dimer is in the form of ADP·P_i. Thus, despite our inability to detect actin-bound hydrolysis products in the present experiments,

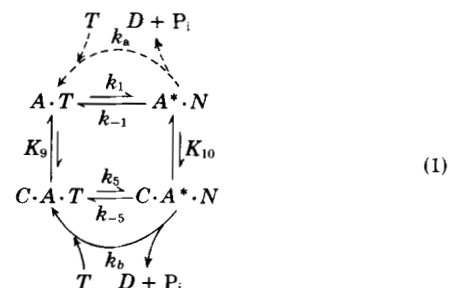
it is possible that the rate-determining step in the cytochalasin-stimulated hydrolysis of ATP is the conformational transition of actin·ADP·P_i.

It is important to realize that cytochalasin stimulates the hydrolysis of ATP by monomeric actin under normal polymerizing conditions and that, as developed in detail by Hill (55), the monomeric ATPase cycle is coupled directly to the monomer-polymer ATPase cycle. The *ACTIN*·NUC* species must, therefore, be considered as possibly an important intermediate in the polymerization of actin when ATP is present. Moreover, irrespective of which of the several monomeric actin species are capable of polymerizing to F-actin, cytochalasins might affect the polymerization process by altering the reaction rates that regulate the formation and breakdown of *ACTIN*·NUC*. These effects of the cytochalasins would be entirely independent of the consequences that result from the very tight binding of cytochalasins to at least one terminus of actin filaments. The very different *K*_{app} values for the interactions of the cytochalasins with monomeric actin could lead to qualitative, as well as quantitative, differences in their effects on actin polymerization.

Acknowledgments—We thank Dr. Evan Eisenberg for valuable discussions throughout the course of this work and for first pointing out the resemblance of our system to the refractory state model for skeletal muscle actomyosin-ATPase activity (53). We also thank Dr. Stephen Mockrin for providing the cross-linked actin dimer and for determining the radiochemical purity of the [α -³²P]ATP.

APPENDIX

To facilitate the steady state kinetic analysis of the model shown in Fig. 6, we rewrite the scheme in the following condensed form, in which *step a* includes steps 2–4 of Fig. 6, and *step b* includes steps 6–8 of Fig. 6:



In this model, the symbols *A*, *C*, *T*, *D*, and *N* represent actin, cytochalasin, ATP, ADP, and nucleotide (or nucleotide + P_i), respectively. The constants *K*₉ and *K*₁₀ are dissociation constants, e.g. *K*₉ = [*C*][*A·T*]/[*C·A·T*]. Following Stein *et al.*

(53), we simplify the model as follows. Define a rate constant k'_1 such that

$$k'_1([A \cdot T] + [C \cdot A \cdot T]) = k_1[A \cdot T] \quad (2)$$

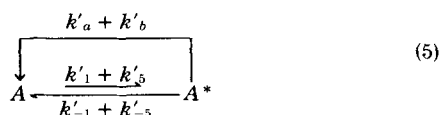
Since $A \cdot T$ and $C \cdot A \cdot T$ are in rapid equilibrium, we have

$$k'_1[A \cdot T] \left(1 + \frac{[C]}{K_9}\right) = k_1[A \cdot T] \quad (3)$$

so that $k'_1 = k_1 K_9 / ([C] + K_9)$. By this reasoning, we generate the series of rate constants:

$$\begin{aligned} k'_{-1} &= \frac{k_{-1} K_{10}}{[C] + K_{10}} & k'_a &= \frac{k_a K_{10}}{[C] + K_{10}} \\ k'_5 &= \frac{k_5 [C]}{[C] + K_9} & k'_b &= \frac{k_b [C]}{[C] + K_{10}} \\ k'_{-5} &= \frac{k_{-5} [C]}{[C] + K_{10}} \end{aligned} \quad (4)$$

Using these definitions, we can write a simplified version of the model (1):



where $[A] = [A \cdot T] + [C \cdot A \cdot T]$ and $[A^*] = [A^* \cdot N] + [C \cdot A^* \cdot N]$. The steady state rate equation for this model is just

$$\begin{aligned} 0 &= \frac{d[A]}{dt} = -\frac{d[A^*]}{dt} \\ &= -[A](k'_1 + k'_5) + [A^*](k'_{-1} + k'_{-5} + k'_a + k'_b) \end{aligned} \quad (6)$$

with the constraint that the total actin concentration $[A]_{\text{tot}} = [A] + [A^*]$. The steady state rate of hydrolysis per mol of total actin is given by $V = (k'_a + k'_b)[A^*]/[A]_{\text{tot}}$ or

$$\frac{1}{V} = \frac{1}{k'_a + k'_b} \left(1 + \frac{[A]}{[A^*]}\right) \quad (7)$$

Substituting Equation 6 into Equation 7, we have

$$\frac{1}{V} = \frac{1}{k'_a + k'_b} \left(1 + \frac{k'_{-1} + k'_{-5} + k'_a + k'_b}{k'_1 + k'_5}\right) \quad (8)$$

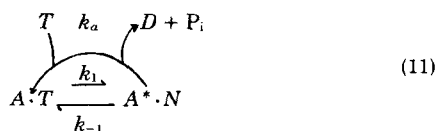
Finally, we substitute the definitions for the primed rate constants given by Equations 4 into Equation 8 and obtain

$$\begin{aligned} \frac{1}{V} &= \frac{[C] + K_{10}}{k_a K_{10} + k_b [C]} + \frac{[C] + K_9}{k_a K_{10} + k_b [C]} \\ &\quad \cdot \frac{(k_{-1} + k_a) K_{10} + (k_{-5} + k_b) [C]}{k_1 K_9 + k_5 [C]} \end{aligned} \quad (9)$$

Let us examine some limiting forms of Equation 9 in order to gain insight into the nature of the rate law. When the cytochalasin concentration approaches zero, the rate becomes

$$V_0 = \frac{k_1 k_a}{k_1 + k_{-1} + k_a} \quad (10)$$

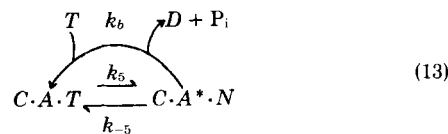
which is the steady state ATP hydrolysis rate for the cycle



If the concentration of cytochalasin is very high, then the rate expression becomes

$$V = \frac{k_5 k_b}{k_5 + k_{-5} + k_b} \quad (12)$$

which is the steady state ATP hydrolysis rate for the cycle with actin always bound to cytochalasin



In the limit that the cytochalasin-stimulated rate k_b is very large, the maximal rate of ATP hydrolysis is limited by the forward rate of the $C \cdot A \cdot T$ to $C \cdot A^* \cdot N$ transition, i.e. $V_{\text{max}} = k_5$.

As shown in Fig. 2, the measured cytochalasin-stimulated monomeric actin ATPases rates yield linear double reciprocal plots when plotted *versus* the total cytochalasin concentration. It is, therefore, useful to rearrange Equation 9 to a double reciprocal form in order to understand the significance of the extrapolated values of V_{max} and K_{app} obtained from such plots. We first assume that no hydrolysis occurs in the absence of cytochalasin because $k_a = 0$. This is a reasonable assumption, since the rate of hydrolysis of ATP is 30–60 times faster in the presence of cytochalasin. For simplicity, we also assume that the cytochalasin dissociation constants K_9 and K_{10} are equal, $K_9 = K_{10} = K$.

With these assumptions, Equation 9 can be regrouped into a constant term, a term proportional to $1/[\text{cytochalasin}]$, and an additional term with a more complicated dependence on the cytochalasin concentration:

$$\begin{aligned} \frac{1}{V} &= \left[\frac{1}{k_1} + \left(1 + \frac{k_{-1}}{k_1}\right) \frac{1}{k_b} \right] \\ &\quad + \frac{1}{[C]} \left[\left(1 + \frac{k_{-1}}{k_1}\right) \frac{K}{k_b} \right] + \frac{[C](k_1 - k_5)}{k_1(k_1 K + k_5 [C])} \end{aligned} \quad (14)$$

In rearranging Equation 9 to obtain Equation 14, we have made use of detailed balance which requires $k_{-1} k_5 = k_1 k_{-5}$. A linear double reciprocal plot will be obtained when the last term in Equation 14 can be neglected. This last term will be identically zero when $k_1 = k_5$ and will approach zero as $[C]$ goes to zero, so that an approximately linear double reciprocal plot is also obtained at relatively low cytochalasin concentrations, even when k_1 does not equal k_5 .

When the last term in Equation 14 can be neglected, we can rewrite this equation in the standard double reciprocal form

$$\frac{1}{V} = \frac{1}{V_{\text{max}}} + \frac{K_{\text{app}}}{V_{\text{max}}} \cdot \frac{1}{[C]}$$

where

$$V_{\text{max}} = \frac{k_1 k_b}{k_1 + k_{-1} + k_b} \quad (15)$$

and

$$K_{\text{app}} = K \left(\frac{k_1 + k_{-1}}{k_1 + k_{-1} + k_b} \right)$$

We, therefore, identify the extrapolated V_{max} and K_{app} values obtained from data such as those in Fig. 2 with the expressions shown in Equation 15.

Let us now consider the limiting forms of V_{max} and K_{app} . If $k_{-1} \gg k_1$ and $k_b \gg k_{-1}$, we find $V_{\text{max}} = k_1$ and $K_{\text{app}} = (k_{-1}/k_b)K$. Thus, V_{max} is determined by a step in which actin is not bound to cytochalasin, and is, therefore, predicted to be the same for any cytochalasin used, while K_{app} depends explicitly on the binding constant, K , for the particular cytochalasin. Note that K_{app} will be much smaller than K , since $k_b \gg k_{-1}$ and that, therefore, the ATPase activity will be titrated at cytochalasin concentrations well below those at which measurable cytochalasin binding occurs.

As the cytochalasin concentration is increased, appreciable

cytochalasin binding occurs, and the last term in Equation 14 cannot be neglected. Under these conditions, the double reciprocal plot will deviate from linearity. As seen in Fig. 4, the resulting double reciprocal plots will be either concave upward or concave downward, depending on whether $k_5 < k_1$ or $k_5 > k_1$, i.e. whether the rate of the $A \cdot T$ to $A^* \cdot N$ transition is faster with unbound or cytochalasin-bound actin monomer. As the cytochalasin concentration becomes very large, the rate becomes

$$\lim_{[C] \rightarrow \infty} \frac{1}{V} = \frac{k_1 + k_{-1} + k_b}{k_1 k_b} + \frac{k_1 - k_5}{k_1 k_5} \quad (16)$$

$$= \frac{k_1 k_5 + k_{-1} k_5 + k_1 k_b}{k_1 k_5 k_b}$$

Note that, as discussed for the general model, if k_b is very large, the maximal rate obtained at very high cytochalasin concentrations approaches k_5 , and the $C \cdot A \cdot T$ to $C \cdot A^* \cdot N$ transition is the rate-determining step. Both at low and high concentrations of cytochalasin, the model predicts that the rate of ATP hydrolysis should be a linear function of the total actin concentration; this is true even on the nonlinear portions of the double reciprocal plots.

REFERENCES

- Korn, E. D. (1978) *Proc. Natl. Acad. Sci. U. S. A.* **75**, 588-599
- Carlsson, L., Nystrom, L. E., Sudkvist, I., Markey, F., and Lindberg, U. (1977) *J. Mol. Biol.* **115**, 465-483
- Reichstein, E., and Korn, E. D. (1979) *J. Biol. Chem.* **254**, 6174-6179
- Blikstad, I., Sundkvist, I., and Eriksson, S. (1980) *Eur. J. Biochem.* **105**, 425-433
- Grumet, M., and Lin, S. (1980) *Cell* **21**, 439-444
- Isenberg, G., Aebi, U., and Pollard, T. D. (1980) *Nature* **288**, 455-459
- Craig, S. W., and Powell, L. D. (1980) *Cell* **22**, 739-746
- Mooseker, M. S., Graves, T. A., Wharton, K. A., Falco, N., and Howe, C. L. (1980) *Cell* **87**, 809-822
- Bretscher, A., and Weber, K. (1980) *Cell* **20**, 839-847
- Hasegawa, T., Takahashi, S., Hayashi, H., and Hatano, S. (1980) *Biochemistry* **19**, 2677-2683
- Norberg, R., Thorstensson, R., Utter, G., and Fagraeus, A. (1979) *Eur. J. Biochem.* **100**, 575-583
- Van Baelen, H., Bouillon, R., and De Moor, P. (1980) *J. Biol. Chem.* **255**, 2270-2272
- Harris, H. E., Bamburg, J. R., and Weeds, A. G. (1980) *FEBS Lett.* **121**, 175-177
- Bamburg, J. R., Harris, H. E., and Weeds, A. G. (1980) *FEBS Lett.* **121**, 178-182
- Maruta, H., and Korn, E. D. (1977) *J. Biol. Chem.* **252**, 399-402
- Tilney, L. G. (1975) *J. Cell Biol.* **64**, 289-310
- Hartwig, J. H., and Stossel, T. P. (1975) *J. Biol. Chem.* **250**, 5696-5705
- Wang, K., and Singer, S. J. (1977) *Proc. Natl. Acad. Sci. U. S. A.* **74**, 2021-2025
- Brenner, S. L., and Korn, E. D. (1979) *J. Biol. Chem.* **254**, 8620-8627
- Kane, R. E. (1976) *J. Cell Biol.* **71**, 704-714
- Mimura, N., and Asano, A. (1979) *Nature* **282**, 44-48
- Yin, H. L., and Stossel, T. P. (1979) *Nature* **281**, 583-586
- Nunnally, M. H., Powell, L. D., and Craig, S. W. (1981) *J. Biol. Chem.* **256**, 2083-2086
- Moore, P. B., Huxley, H. E., and DeRosier, D. J. (1970) *J. Mol. Biol.* **50**, 279-295
- Collins, J. H., and Elzinga, M. (1975) *J. Biol. Chem.* **250**, 5915-5920
- Neidl, C., and Engel, J. (1979) *Eur. J. Biochem.* **101**, 163-169
- Martonosi, A., Molino, C. M., and Gergely, J. (1964) *J. Biol. Chem.* **239**, 1057-1064
- Frieden, C., Lieberman, D., and Gilbert, H. R. (1980) *J. Biol. Chem.* **255**, 8991-8993
- Straub, F. B., and Feuer, G. (1950) *Biochim. Biophys. Acta* **4**, 455-470
- Cooke, R. (1975) *Biochemistry* **14**, 3250-3256
- Brenner, S. L., and Korn, E. D. (1980) *J. Biol. Chem.* **255**, 841-844
- Pardee, J. D., and Spudich, J. A. (1980) *J. Cell Biol.* **87**, 226a
- Mockrin, S. C., and Korn, E. D. (1981) *J. Biol. Chem.* **256**, 8228-8232
- Hayashi, T., and Rosenbluth, R. (1960) *Biol. Bull. (Woods Hole)* **119**, 290
- Cooke, R., and Murdoch, L. (1973) *Biochemistry* **12**, 3927-3932
- Wegner, A. (1976) *J. Mol. Biol.* **108**, 139-150
- Tanenbaum, S. W. (1978) *Cytochalasins: Biochemical and Cell Biological Aspects*, Elsevier/North Holland, Amsterdam
- Brenner, S. L., and Korn, E. D. (1979) *J. Biol. Chem.* **254**, 9982-9985
- Brown, S. S., and Spudich, J. A. (1980) *J. Cell Biol.* **83**, 657-662
- Lin, D. C., Tobin, K. D., Grumet, M., and Lin, S. (1980) *J. Cell Biol.* **84**, 455-460
- MacLean-Fletcher, S., and Pollard, T. D. (1980) *Cell* **20**, 329-341
- Hartwig, J. H., and Stossel, T. P. (1979) *J. Mol. Biol.* **134**, 539-553
- Löw, I., Dancker, P., and Wieland, T. (1975) *FEBS Lett.* **54**, 263-265
- Löw, I., and Dancker, P. (1976) *Biochim. Biophys. Acta* **430**, 366-374
- Selden, L. A., Gershman, L. C., and Estes, J. E. (1980) *Biochem. Biophys. Res. Commun.* **95**, 1854-1860
- Estes, J. E., Selden, L. A., and Gershman, L. C. (1981) *Biophys. J.* **33**, 24a
- Pollard, T. D., and Korn, E. D. (1973) *J. Biol. Chem.* **248**, 4682-4690
- Spudich, J. A., and Watt, S. (1971) *J. Biol. Chem.* **246**, 4866-4871
- Eisenberg, E., and Kielley, W. W. (1974) *J. Biol. Chem.* **249**, 4742-4748
- Gordon, D., Eisenberg, E., and Korn, E. D. (1976) *J. Biol. Chem.* **251**, 4778-4786
- Gordon, D., Yang, Y.-Z., and Korn, E. D. (1976) *J. Biol. Chem.* **251**, 7474-7479
- Lowry, O. H., Rosebrough, N. J., Farr, A. L., and Randall, R. J. (1951) *J. Biol. Chem.* **193**, 265-275
- Stein, L. A., Schwarz, R. P., Chock, P. B., and Eisenberg, E. (1979) *Biochemistry* **18**, 3895-3909
- Ferri, A., Magri, E., and Grazi, E. (1979) *Biochem. J.* **183**, 475-476
- Hill, T. L. (1980) *Proc. Natl. Acad. Sci. U. S. A.* **77**, 4803-4807